

Pentanuclear Heterometallic $\{Ni_2Ln_3\}$ ($Ln = Gd, Dy, Tb, Ho$) Assemblies. Single-Molecule Magnet Behavior and Multistep Relaxation in the Dysprosium Derivative

Vadapalli Chandrasekhar,^{*,†,‡} Prasenjit Bag,[†] Wolfgang Kroener,[§] Klaus Gieb,[§] and Paul Müller[§]

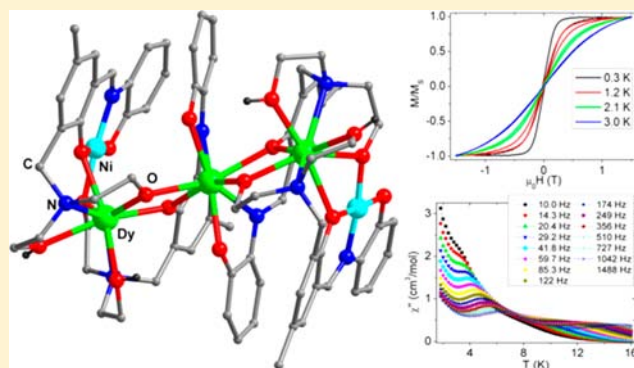
[†]Department of Chemistry, Indian Institute of Technology Kanpur, Kanpur 208016, India

[‡]Tata Institute of Fundamental Research, Centre for Interdisciplinary Sciences, 21 Brundavan Colony, Narsingi, Hyderabad 500075, India

[§]Department of Physics, Universität Erlangen-Nürnberg, Erwin-Rommel-Straße 1, D-91058 Erlangen, Germany

Supporting Information

ABSTRACT: The reaction between Ln(III) chloride and $NiCl_2 \cdot 4H_2O$ salts in presence of a multidentate sterically unencumbered ligand, (*E*)-2,2'-(2-hydroxy-3-((2-hydroxyphenylimino)methyl)-5-methylbenzylazanediyl)diethanol (LH_4) leads to the synthesis of four isostructural pentanuclear heterometallic complexes $[Ni_2Dy_3(LH_4)_4]Cl$ (**1**), $[Ni_2Gd_3(LH_4)_4]Cl$ (**2**), $[Ni_2Tb_3(LH_3)(LH_2)]Cl_2$ (**3**), $[Ni_2Ho_3(LH_3)(LH_2)]Cl_2$ (**4**) with unprecedented topology. Here the two compounds **1** are **2** are monocationic and crystallize in chiral space group, $P2_12_12_1$ whereas compounds **3** and **4** are dicationic and crystallize in achiral space group $P2_1/n$. The total metal framework, $\{Ni_2Ln_3\}$ unit is held by four triply deprotonated ligands $[LH]^{3-}$ in **1** and **2** whereas in case of **3** and **4** three triply deprotonated $[LH]^{3-}$ and one doubly deprotonated $[LH_2]^{2-}$ ligands are involved. In these complexes both the lanthanide ions and the nickel(II) ions are doubly bridged and the bridging is composed of oxygen atoms derived from either phenolate or ethoxide groups. The analysis of SQUID measurements reveal a high magnetic ground state and a slow relaxation of the magnetization with two relaxation regimes for **1**. For the thermally activated regime we found an effective energy barrier of $U_{eff} = 85$ K. Micro Hall probe loop measurements directly proof the single-molecule magnet (SMM) nature of **1** with a blocking temperature of $T_B = 3$ K and an open hysteresis for sweep rates faster than 50 mT/s.



both the lanthanide ions and the nickel(II) ions are doubly bridged and the bridging is composed of oxygen atoms derived from either phenolate or ethoxide groups. The analysis of SQUID measurements reveal a high magnetic ground state and a slow relaxation of the magnetization with two relaxation regimes for **1**. For the thermally activated regime we found an effective energy barrier of $U_{eff} = 85$ K. Micro Hall probe loop measurements directly proof the single-molecule magnet (SMM) nature of **1** with a blocking temperature of $T_B = 3$ K and an open hysteresis for sweep rates faster than 50 mT/s.

INTRODUCTION

Mixed metal complexes, especially those that contain 3d/4f metal ions, are gaining importance in view of their interesting magnetic properties.¹ Some of these compounds, possessing a high spin ground state (*S*), high uniaxial magnetic anisotropy (*D*), and negligible intermolecular magnetic interactions have shown single-molecule magnet (SMM) behavior at low temperatures.² Initially such studies were limited to $Cu^{II}/4f$ metal ion complexes.³ However, these studies soon expanded to compounds containing other types of transition metal ions, particularly Mn^{III} ,⁴ Fe^{III} and Co^{II} .⁶ Interestingly 3d/4f compounds containing Ni^{II} have been relatively few,⁵ in spite of the fact that considerable magnetic anisotropy generated from second order orbital angular momentum in $Ni(II)$ ion makes it worthwhile to incorporate this ion in heterometallic 3d-4f compounds. We have been interested in the use of phosphorus-supported ligands in assembling homo- and heterometallic complexes. Thus, we showed that by using $SP[N(Me)N=CH-C_6H_3-2-OH-3-OMe]_3$ (LH_3) we could prepare linear trinuclear heterometallic complexes containing Co^{II} -

Ln^{III} - Co^{II} and Ni^{II} - Ln^{III} - Ni^{II} cores, many of which were shown to be SMMs.⁸ We realized that the above ligand in spite of its versatility is limited to generating only trinuclear systems. A perusal of the literature revealed that a Schiff base ligand generated from *o*-vanillin and 2-aminophenol successfully facilitates the assembly of polynuclear heterometallic complexes possessing interesting magnetic properties.⁹ Among these is a $\{Co(II)_2Dy_2\}$ complex which shows the highest energy barrier (117 K) for magnetization reversal for any 3d-4f complex reported so far.^{9b} This spurred us to design a new chelating, flexible, multisite coordinating ligand, (*E*)-2,2'-(2-hydroxy-3-((2-hydroxyphenylimino)methyl)-5-methylbenzylazanediyl)-diethanol (LH_4). Utilizing this ligand we have been able to assemble both mono cationic and dicationic pentanuclear heterometallic $\{Ni_2Ln_3\}$ complexes [$Ln(III) = Dy$ (**1**), Gd (**2**), Tb (**3**), Ho (**4**)]. While two of these complexes crystallize in the chiral space group $P2_12_12_1$, the other two crystallize in the

Received: July 23, 2013

Published: November 7, 2013

Table 1. Details of the Data Collection and Refinement Parameters for Compounds 1–4

	1	2	3	4
formula	C ₇₈ H ₉₂ N ₈ O ₁₈ Cl Ni ₂ Dy ₃	C ₇₉ H ₉₈ N ₈ O ₂₀ Cl Ni ₂ Gd ₃	C ₇₈ H ₉₂ N ₈ O ₁₈ Cl ₅ Ni ₂ Tb ₃	C ₈₁ H ₁₀₅ N ₈ O ₂₁ Cl ₂ Ni ₂ Ho ₃
M/g	2069.97	2104.27	2201.03	2209.84
crystal system	orthorhombic	orthorhombic	monoclinic	monoclinic
space group	<i>P</i> 2 ₁ 2 ₁ 2 ₁	<i>P</i> 2 ₁ 2 ₁ 2 ₁	<i>P</i> 2 ₁ / <i>n</i>	<i>P</i> 2 ₁ / <i>n</i>
wavelength (MoK α)	0.71073	0.71073	0.71073	0.71073
unit cell dimensions (Å, deg)	<i>a</i> = 13.0205(5) <i>b</i> = 22.8391(9) <i>c</i> = 26.1866(10) α = 90 γ = 90 β = 90	<i>a</i> = 13.044(1) <i>b</i> = 26.228(2) <i>c</i> = 22.883(2) α = 90 β = 90 γ = 90	<i>a</i> = 13.198(3) <i>b</i> = 26.420(5) <i>c</i> = 23.571(5) α = 90 γ = 90 β = 90.52(3)	<i>a</i> = 13.325(9) <i>c</i> = 23.143(2) <i>b</i> = 26.546(2) α = 90 γ = 90 β = 90.366(2)
V/Å ³	7787.3(5)	7829.5(10)	8219(3)	8186.2(10)
Z	4	4	4	4
ρ_c /g cm ⁻³	1.766	1.785	1.779	1.793
μ /mm ⁻¹	3.427 mm ⁻¹	3.091	3.233	3.461
F(000)	4124	4212	4384	4424
cryst size (mm ³)	0.12 × 0.105 × 0.085	0.125 × 0.105 × 0.09	0.105 × 0.09 × 0.075	0.11 × 0.10 × 0.085
θ range (deg)	1.18 to 25.50°	1.74 to 25.50	1.16 to 25.50	1.17 to 25.50°
limiting indices	-13 ≤ <i>h</i> ≤ 15, -20 ≤ <i>k</i> ≤ 27, -29 ≤ <i>l</i> ≤ 31	-15 ≤ <i>h</i> ≤ 15, -31 ≤ <i>k</i> ≤ 29, -25 ≤ <i>l</i> ≤ 27	-15 ≤ <i>h</i> ≤ 15, -32 ≤ <i>k</i> ≤ 30, -20 ≤ <i>l</i> ≤ 28	-16 ≤ <i>h</i> ≤ 11, -32 ≤ <i>k</i> ≤ 27, -27 ≤ <i>l</i> ≤ 28
reflns collected	42591	42948	43569	44232
ind reflns	14468 [R(int) = 0.0733]	14537 [R(int) = 0.1010]	15220 [R(int) = 0.1198]	15199 [R(int) = 0.0845]
completeness to θ (%)	99.9	99.9	99.6	99.8
refinement method	full-matrix-block least-squares on F ²	full-matrix-block least-squares on F ²	full-matrix-block least-squares on F ²	full-matrix-block least-squares on F ²
data/restraints/params	14468/200/957	14537/81/1043	15220/85/1052	15199/58/1084
goodness-of-fit on F ²	1.055	0.996	1.067	1.031
final R indices [<i>I</i> > 2 θ (<i>I</i>)]	<i>R</i> 1 = 0.0505, <i>w</i> R2 = 0.1212	<i>R</i> 1 = 0.0586, <i>w</i> R2 = 0.1244	<i>R</i> 1 = 0.0871, <i>w</i> R2 = 0.2089	<i>R</i> 1 = 0.0634, <i>w</i> R2 = 0.1617
R indices (all data)	<i>R</i> 1 = 0.0685, <i>w</i> R2 = 0.1364	<i>R</i> 1 = 0.0966, <i>w</i> R2 = 0.1526	<i>R</i> 1 = 0.1456, <i>w</i> R2 = 0.2408	<i>R</i> 1 = 0.1148, <i>w</i> R2 = 0.1969
absolute structure parameter	-0.025(14)	-0.032(18)		
largest diff. peak and hole(e Å ⁻³)	2.056 and -0.832	1.678 and -3.601	2.295 and -1.913	2.037 and -4.553

achiral space group *P*2₁/*n*. The details of magnetic analysis shows that compound **1** possesses a ferromagnetic ground state while an antiferromagnetic ground state is observed for **2**, **3**, and **4**. A clear appearance of multistep relaxation path way can be delineated from the out of phase *ac*-susceptibility signal of **1** with thermally activated regime; we found an effective energy barrier of $U_{\text{eff}} = 85$ K. This is the by a very great margin largest energy barrier among the Ni/Ln complexes reported so far. These results are discussed herein.

EXPERIMENTAL SECTION

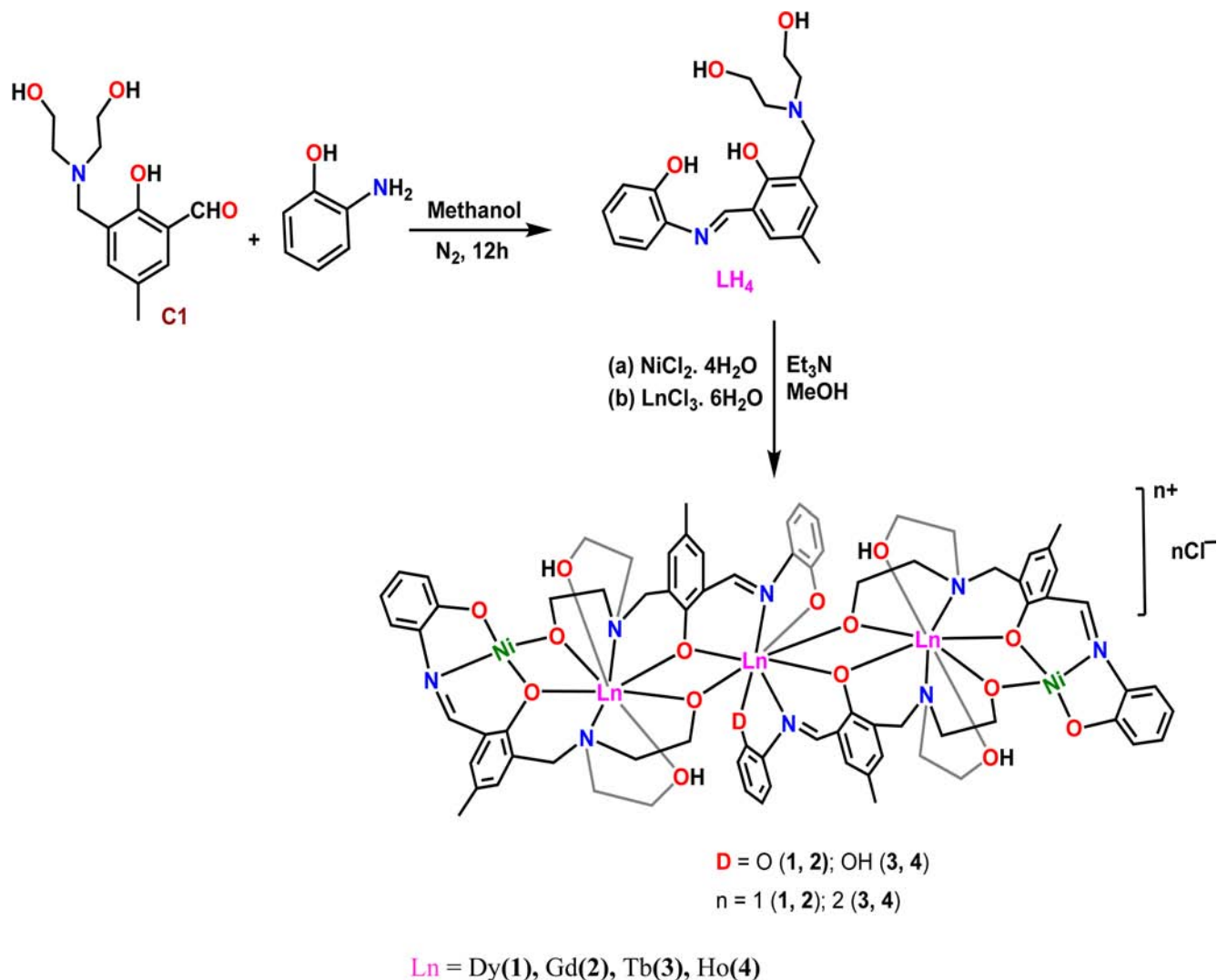
Reagents and General Procedures. Solvents and other general reagents used in this work were purified according to standard procedures.¹⁰ Anhydrous magnesium chloride (Alfa Aesar, Hyderabad, India) was used as purchased. Diethanolamine, *p*-cresol, paraformaldehyde, 2-aminophenol, and NiCl₂·4H₂O were obtained from SD Fine Chemicals, Mumbai, India, and were used as received. LnCl₃·6H₂O were obtained from Aldrich Chemical Co., U.S.A and were used without further purification. 3-((Bis(2-hydroxyethyl)amino)methyl)-2-hydroxy-5-methylbenzaldehyde (**C1**),¹¹ was synthesized according to literature procedure.

Instrumentation. Melting points were measured using a JSGW melting point apparatus and are uncorrected. IR spectra were recorded as KBr pellets on a Bruker Vector 22 FT IR spectrophotometer operating between 400–4000 cm⁻¹. ¹H NMR was recorded on a JEOL-JNM LAMBDA model 400 spectrometer using CD₃OD

operating at 400 MHz. Elemental analyses of the compounds were obtained from Thermoquest CE instruments CHNS-O, EA/110 model. Electrospray ionization mass spectrometry (ESI-MS) spectra were recorded on a Micromass Quattro II triple quadrupole mass spectrometer. Electrospray ionization (positive ion, full scan mode) was used keeping methanol as the solvent for desolvation. Capillary voltage was maintained at 2 kV, and cone voltage was kept at 31 kV.

The magnetic direct current (*dc*) and alternating current (*ac*) susceptibility were recorded with a commercial superconducting quantum interference device (SQUID) magnetometer from Quantum Design (MPMS-XL) equipped with a 5 T magnet, a *dc* transport unit, and an *ac* susceptibility measurement unit. The analysis of the SQUID data was performed with the program DAVE.¹² Low temperature hysteresis loop measurements were performed with a custom Hall probe magnetometer.¹³ A 8 T magnet was used for the external field and a Heliox ³He cryostat from Oxford Instruments was used to cool the sample down to mK temperatures.

Syntheses. (*E*)-2,2'-(2-hydroxy-3-((2-hydroxyphenylimino)methyl)-5-methylbenzylazanediyl)diethanol (**LH₄**). **C1** (2.54 g, 1.0 mmol) was taken in 15 mL of methanol and added dropwise to a solution of 2-aminophenol (1.09 g, 1.0 mmol) taken in dry methanol (15 mL). The resulting solution was stirred for 12 h under N₂ atmosphere. Then, the solution was evaporated to dryness and washed 3–4 times with 5–6 mL of dichloromethane to give **LH₄** as a yellowish-orange solid. Yield: 2.45 g, 71.50%. Mp: 130 °C. IR (KBr) cm⁻¹: 3426 (s), 3224 (m), 3065 (w), 2946 (s), 2832 (s), 1618 (s), 1582 (s), 1506 (m), 1461 (s), 1376 (s), 1262 (s), 1245 (s), 1125 (m), 1109 (m), 1054 (s), 1046 (s). ¹H NMR (CD₃OD, δ , ppm): 8.82 (s, 1H,

Scheme 1. Synthesis of the Ligand (LH₄) and Metal Complexes 1–4

–CH=N), 7.24(m, 3H, Ar–H), 7.08(s, 1H, Ar–H), 6.87(m, 2H, Ar–H), 3.62 (t, 4H, CH₂O), 3.76 (s, 2H, ArCH₂), 2.70 (t, 4H, NCH₂), 2.28 (s, 3H, ArCH₃). ESI-MS (*m/z*): 345.18, [M+H]⁺. Anal. Calcd for C₁₉H₂₄N₂O₄: C, 66.26; H, 7.02; N, 8.13. Found: C, 66.07; H, 6.88; N, 7.98.

Preparation of the Pentanuclear Complexes 1–4. A general synthetic protocol was applied for the preparation of all the metal complexes (1–4) as follows. LH₄ (0.052 g, 0.15 mmol) was dissolved in methanol (20 mL). LnCl₃·6H₂O (0.037 g, 0.10 mmol) and triethylamine (0.06 mL, 0.45 mmol) were added to this solution. The reaction mixture was stirred for 1 h. At this stage, NiCl₂·4H₂O (0.023 g, 0.10 mmol) was added, and the reaction mixture was stirred for a further period of 3 h at room temperature to afford a clear solution. A red-colored solution was obtained which was evaporated in vacuo, not allowing the bath temperature to exceed 40 °C, affording a powder which was then washed with diethyl ether. X-ray quality crystals of 1–4 were grown by vapor diffusion of diethyl ether into the mixture of methanol/chloroform (1:1 v/v) solution of the corresponding complex. The characterization data for these complexes are given below.

[Ni₂Dy₃(LH)₄]Cl₂·3CH₃OH (1). Yield: 0.029 g, 41.92% (based on Dy). Mp: >230 °C. IR (KBr) cm⁻¹: 3407 (b), 2909 (m), 2847 (m), 1602 (s), 1585 (s), 1561(s), 1478 (s), 1375 (s), 1309 (s), 1252 (m), 1172 (s), 1149 (m), 1093 (s), 1074 (s). ESI-MS *m/z*, ion: 1970.27, [M]⁺. Anal. Calcd C₇₈H₉₂N₈O₁₈ClNi₂Dy₃ (2069.97): C, 45.26; H, 4.48; N, 5.41. Found: C, 45.02; H, 4.26; N, 5.24.

[Ni₂Gd₃(LH)₄]Cl₂·3CH₃OH·H₂O (2). Yield: 0.026 g, 36.61% (based on Gd). Mp: >230 °C. IR (KBr) cm⁻¹: 3403 (b), 2910 (m), 2842 (m), 1603 (s), 1585 (s), 1558(s), 1478 (s), 1376 (s), 1309 (s), 1252 (m), 1172 (s), 1150 (m), 1092 (s), 1073 (s). ESI-MS *m/z*, ion: 1955.25, [M]⁺. Anal. Calcd C₇₉H₉₈N₈O₂₀ClNi₂Gd₃ (2104.27): C, 45.09; H, 4.69; N, 5.33. Found: C, 44.80; H, 4.45; N, 5.26.

[Ni₂Tb₃(LH)₃(LH₂)]Cl₂·CHCl₃·CH₃OH·H₂O (3). Yield: 0.030 g, 40.17% (based on Tb). Mp: >230 °C. IR (KBr) cm⁻¹: 3410 (b), 2908 (m), 2842 (m), 1603 (s), 1585 (s), 1558(s), 1478 (s), 1376 (s), 1309 (s), 1252 (m), 1172 (s), 1150 (m), 1092 (s), 1073 (s). ESI-MS *m/z*, ion: 980.12, [M]²⁺. Anal. Calcd C₇₈H₉₂N₈O₁₈Cl₃Ni₂Tb₃ (2201.03): C, 42.56; H, 4.21; N, 5.09. Found: C, 42.27; H, 4.06; N, 4.96.

[Ni₂Ho₃(LH)₃(LH₂)]Cl₂·5CH₃OH (4). Yield: 0.026 g, 34.67% (based on Ho). Mp: >220 °C. IR (KBr) cm⁻¹: 3406 (b), 2910 (m), 2845 (m), 1603 (s), 1585 (s), 1559(s), 1479 (s), 1376 (s), 1310 (s), 1268 (m), 1172 (s), 1132 (s), 1092 (s), 1073 (s). ESI-MS *m/z*, ion: 989.13, [M]²⁺. Anal. Calcd C₈₁H₁₀₅N₈O₂₁Cl₂Ni₂Ho₃ (2209.84): C, 44.02; H, 4.79; N, 5.07. Found: C, 43.81; H, 4.59; N, 4.93.

X-ray Crystallography. The crystal data and the cell parameters for 1–4 are given in Table 1. The crystal data were collected on a Bruker SMART CCD diffractometer using a Mo K α sealed tube. The program SMART^{14a} was used for collecting frames of data, indexing reflections, and determining lattice parameters, SAINT^{14a} for integration of the intensity of reflections and scaling, SADABS^{14b} for absorption correction, and SHELXTL^{14c,d} for space group and structure determination and least-squares refinements on F². All the

structures were solved by direct methods using the programs SHELXS-97^{14e} and refined by full-matrix least-squares methods against F^2 with SHELXL-97.^{14e} Hydrogen atoms were fixed at calculated positions, and their positions were refined by a riding model. All non-hydrogen atoms were refined with anisotropic displacement parameters. The crystallographic figures used in this manuscript have been generated using Diamond 3.1e software.¹⁴

RESULTS AND DISCUSSION

Synthetic Aspects. The synthesis of the ligand LH_4 involved direct condensation of 3-((bis(2-hydroxyethyl)amino)methyl)-2-hydroxy-5-methylbenzaldehyde (C1) with 2-aminophenol in methanol (Scheme 1). ESI-MS of LH_4 revealed prominent parent ion peaks at m/z 345.18. The ligand, LH_4 comprises two coordination compartments; one of these contains two phenolic oxygen and one imino nitrogen atoms (chelating ONO donor; site 1). The other compartment consists of a phenolic oxygen and a flexible diethanolamine group (tetradentate OONO donor; site 2). The latter is some what reminiscent of the *scorpionate* type binding cavity present in trispyrazolyl borates (Figure 1). Thus, potentially LH_4 has 6



Figure 1. Two distinct coordination compartments of LH_4 . Site 1 contains a chelating ONO coordination manifold while Site 2 provides a *scorpionate*-like binding cavity.

coordination sites; all of them would be expected to participate in coordination to afford heterometallic ensembles. There is literature precedence that lends support to the design of our ligand for the purpose of incorporating both 3d and 4f metal ions in the same compound. Thus, previously a ligand synthesized from *o*-vanillin and 2-aminophenol has been shown to be effective for the preparation of 3d/4f compounds that possess interesting magnetic properties.⁹ In LH_4 , while retaining the aminophenol platform we modified the *o*-vanillin part to include the flexible diethanolamine side arm with the expectation that this unit will facilitate binding of lanthanide ions. Also, we envisaged that while the free form of LH_4 can function as a terminal ligand, its deprotonated form can facilitate the expansion of the metal ensemble through its bridging coordination action. In accordance with all the above expectations, the multisite coordinating Schiff base ligand LH_4 reacted with $NiCl_2 \cdot 4H_2O$ and $LnCl_3 \cdot 6H_2O$ in a 1.5:1:1 stoichiometric ratio, in the presence of triethylamine as the base in methanol, to afford the heterometallic pentanuclear mono cationic $[Ni_2Ln_3(LH)_4]Cl$ (1, 2) and the dicationic complex salts $[Ni_2Ln_3(LH)_3(LH_2)]Cl_2$ (3, 4) in moderate yields (Scheme 1; see Experimental Section for synthetic details). The molecular structures of all of these compounds were determined by single-crystal X-ray crystallography (vide infra). 1–4 retain their molecular integrity in solution as evidenced by the detection of prominent molecular ion peaks in

their ESI-MS spectra (see Experimental Section and Supporting Information).

X-ray Crystallography. Crystals suitable for X-ray analysis were grown over a week by vapor diffusion of diethyl ether into the solution of the corresponding complex in a 1:1 (v/v) mixture of methanol and chloroform. Single crystal X-ray analysis reveals 1 and 2 crystallize in the chiral space group $P2_12_12_1$ while 3, 4 crystallize in the monoclinic space group $P2_1/n$. The asymmetric unit of 1–4 consists of a full molecule, namely, $[Ni_2Ln_3(LH)_4]Cl$ (1, 2), $[Ni_2Ln_3(LH)_3(LH_2)]Cl_2$ (3, 4) respectively. The refined Flack parameters of 1, 2 are $-0.025(14)$, $-0.032(18)$ respectively indicating the crystallization of enantiopure forms. However, for the bulk sample, circular dichroism experiments failed to produce any signal. This is probably due to the presence of a conglomerate (racemic mixture of crystals of the two enantiomers that crystallize out separately).¹⁵

Compounds 1 and 2 are isomorphous and monocationic. The pentanuclear core of the complexes contains a central linear trinuclear $\{Ln_3\}$ unit either end of which supports a Ni(II). In view of the structural similarity of 1 and 2 we have chosen complex $[Ni_2Dy_3(LH)_4]^+$ (1) as the representative example to describe the overall structure. The structural features of this compound are detailed in Figures 2–6. Selected

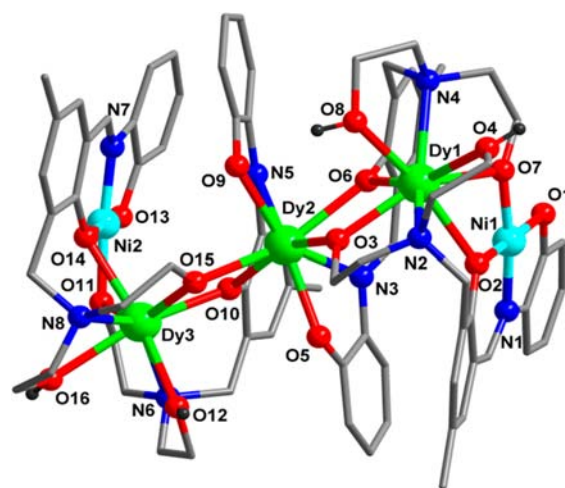


Figure 2. Molecular Structure of 1, hydrogen atoms on carbon, counteranions, and solvent molecules were omitted for clarity. Selected bond distances (Å) and bond angles (deg) are as follows: $Dy(3)-Dy(2) = 3.861(7)$, $Dy(2)-Dy(1) = 3.843(1)$, $Dy(3)-Ni(2) = 3.202(2)$, $Dy(1)-Ni(1) = 3.214(2)$, $Ni(1)-O(2)-Dy(1) = 98.8(3)$, $Ni(1)-O(7)-Dy(1) = 100.3(3)$, $Dy(1)-O(6)-Dy(2) = 109.6(3)$, $Dy(1)-O(3)-Dy(2) = 112.9(3)$, $Dy(3)-O(15)-Dy(2) = 114.8(3)$, $Dy(3)-O(10)-Dy(2) = 110.1(3)$, $Ni(2)-O(11)-Dy(3) = 99.9(3)$, $Ni(2)-O(14)-Dy(3) = 97.6(3)$, $Ni(2)-Dy(3)-Dy(2) = 91.80(3)$, $Ni(1)-Dy(1)-Dy(2) = 90.39(3)$, $Dy(1)-Dy(2)-Dy(3) = 164.60(2)$.

bond parameters of 1 are summarized in the caption of Figures 2–5. The molecular structures and selected bond parameters of the other compounds (2–4) are given in the Supporting Information, Figures S6–S8, Tables S1–S3.

The formation of 1 involves four triply deprotonated $[LH]^{3-}$ ligands, two of which are present in the center and two others in the termini. The pentanuclear core consists of two terminal $[NiDyO_2]$ and two central $[Dy_2O_2]$ four-membered rings; remarkably all these are contiguous with each other. This interconnected multiring system represents a unique structural

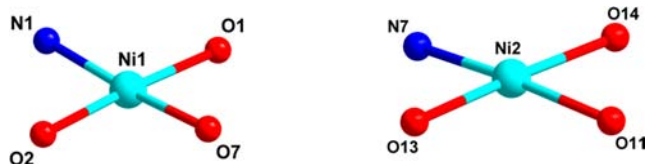


Figure 3. (a) Square planar geometry around the Ni(1) and Ni(2) ions in **1**. Selected bond distances (Å) are as follows: Ni(1)–N(1) = 1.832(9), Ni(1)–O(2) = 1.844(7), Ni(1)–O(1) = 1.853(8), Ni(1)–O(7) = 1.878(8), Ni(2)–O(13) = 1.833(8), Ni(2)–O(14) = 1.852(7), Ni(2)–N(7) = 1.865(9), Ni(2)–O(11) = 1.870(8).

feature which is different from those found in other Ni^{II}/Ln based systems reported so far.⁷ The three dysprosium ions, Dy1, Dy2, and Dy3, form the spirocyclic centers of two of these four-membered rings (Figures 2, 6). The oxygen atoms of these four-membered rings are derived from a phenolate ligand and a deprotonated *N*-ethanol side chain. Each of the two nickel(II) ions are surrounded by a similar coordination environment (3O, 1N) and both possess a rare square planar geometry (Figure 3). The coordination around Ni(II) involves Site 1 of the ligand (N1, O1, O2) along with the *N*-ethoxide (O7). Among the three lanthanide ions the central lanthanide (Dy2) possesses a slightly different coordination environment vis-à-vis the other two. Thus although Dy1, Dy2, and Dy3 are all octacoordinate (2N, 6O), Dy1 and Dy3 possess a $-\text{[CH}_2\text{-CH}_2\text{-OH]}$ ligand in their coordination environment. Also, while Dy1 and 3 are in a distorted trigonal dodecahedral geometry Dy2 is present in a square-antiprism geometry (Figures 4 and 5). To determine the coordination geometry around each Dy(III) ion we have calculated skew angle (φ), intraplanar distance (d_{ip}), interplanar distances (d_{pp}) along with the dihedral angle between the two mean plane (θ) defined by the neighboring ligand donor sites (Supporting Information, Table S5, Figure S15). For an ideal square antiprism geometry (D_{4d} symmetry) the d_{ip} and d_{pp} almost should be equal and φ must be close to 45° .¹⁶ Also θ should be close to zero then the two mean planes will be parallel. The data in Supporting Information, Table S5 supports the distorted square antiprism geometry around Dy2. In case of Dy1 and Dy3 these values are far from D_{4d} symmetry and also each set of coordinating atoms (O2, O7, N2, O4 and O3, O6, N4, O8) around Dy1 deviate away from planarity as can be seen in Supporting Information, Figure S15. Therefore, it is suggested Dy1 and Dy3 possess a distorted trigonal dodecahedron geometry around them. The

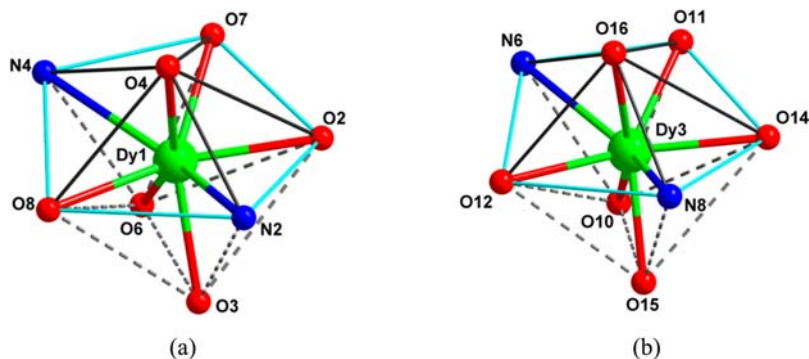


Figure 4. Distorted trigonal-dodecahedron environment around the Dy1 (a) and Dy3 (b) in **1**. Selected bond distances (Å) are as follows: Dy(1)–O(3) = 2.272(7), Dy(1)–O(7) = 2.293(7), Dy(1)–O(6) = 2.309(7), Dy(1)–O(2) = 2.366(8), Dy(1)–O(8) = 2.394(7), Dy(1)–O(4) = 2.439(8), Dy(1)–N(4) = 2.584(9), Dy(1)–N(2) = 2.586(9), Dy(2)–O(15) = 2.314(7), Dy(2)–O(5) = 2.331(7), Dy(2)–O(3) = 2.338(7), Dy(2)–O(9) = 2.347(7), Dy(2)–O(6) = 2.394(7), Dy(2)–O(10) = 2.414(7), Dy(2)–N(3) = 2.507(9), Dy(2)–N(5) = 2.521(9).

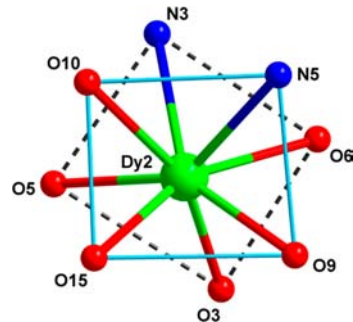


Figure 5. Distorted square antiprism geometry around the Dy2. Selected bond distances (Å) are as follows: Dy(2)–O(15) = 2.314(7), Dy(2)–O(5) = 2.331(7), Dy(2)–O(3) = 2.338(7), Dy(2)–O(9) = 2.347(7), Dy(2)–O(6) = 2.394(7), Dy(2)–O(10) = 2.414(7), Dy(2)–N(3) = 2.507(9), Dy(2)–N(5) = 2.521(9).

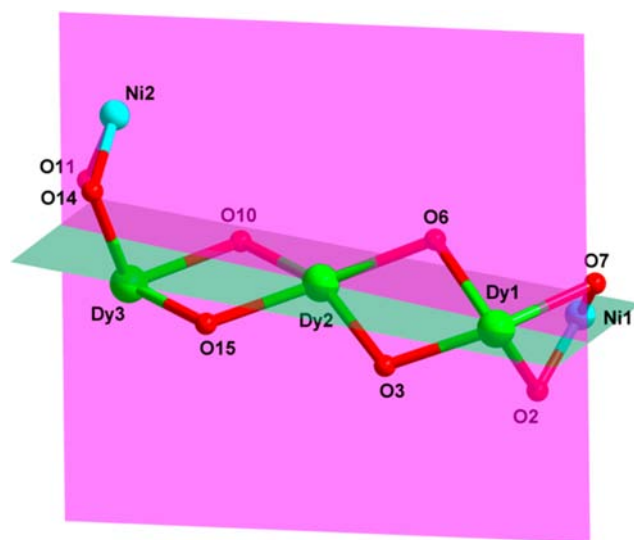


Figure 6. Ni₂Dy₃ of **1** showing the arrangement of the two planes, each of them constitute with a {Dy₃} unit and one of the Ni(II) ions.

bond parameters of **1** are summarized in the caption of Figure 2 and are consistent with literature precedents on Ni–O, Ni–N, Dy–O, and Dy–N bond distances.¹⁷

An interesting feature of the molecular structure of **1** is that all the three Dy(III) ions are arranged in a near-linear fashion

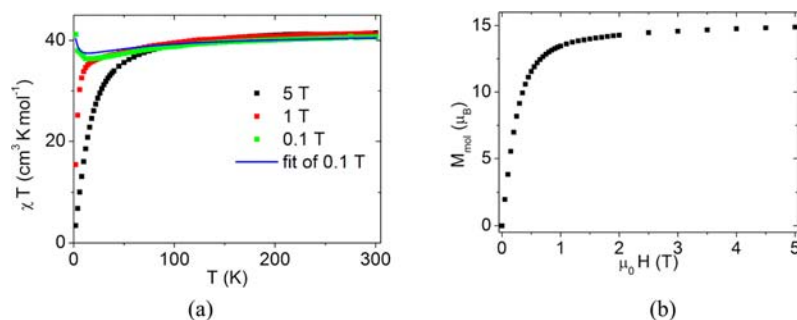


Figure 7. (a) *dc* susceptibility vs temperature of **1**; (b) magnetization measurement $M(H)$ at 1.8 K of **1**.

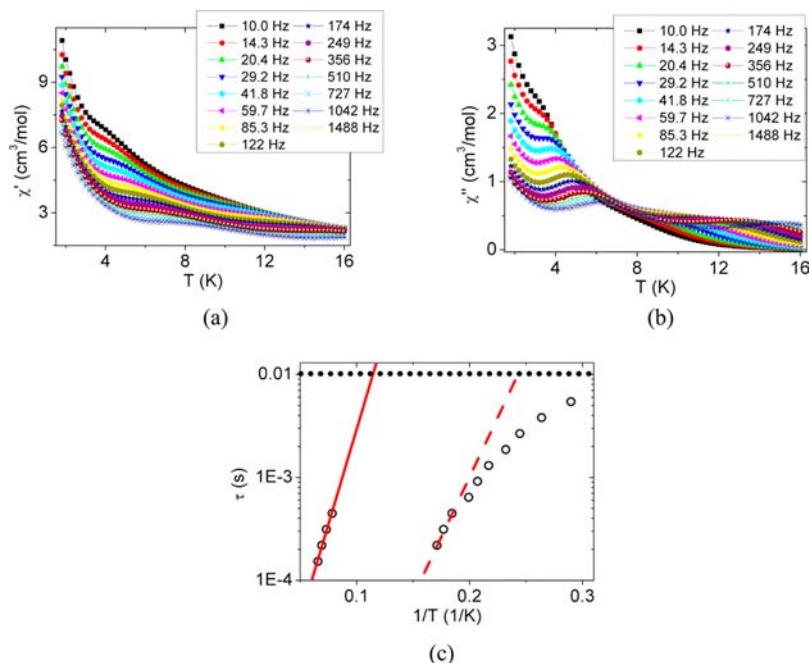


Figure 8. (a) In phase signal of an *ac* measurement of **1**; (b) out of phase signal of the same measurement; (c) Arrhenius plot with data extracted from (b), the estimated low temperature relaxation is depicted as dotted line.

with a Dy...Dy...Dy angle of 164.6° and with inter Dy...Dy distances of 3.843(1) (Dy1–Dy2), 3.861(7) (Å) (Dy2–Dy3) and 7.635(12) (Dy1–Dy3) Å. The two Ni(II) ions are displaced on either side of the trinuclear Dy₃ core with Ni...Dy bond distances of 3.202(2) and 3.214(2) Å (Figures 2, 6). Overall, in the pentanuclear assembly of **1**, the two planes [Ni(1)–Dy(1)–Dy(2)–Dy(3)] and [Dy(1)–Dy(2)–Dy(3)–Ni(2)] are almost perpendicular to each other (Figure 6).

The crystal structure of **1** reveals the formation of a supramolecular polymeric association along the crystallographic *a*-axis through intermolecular O–H...Cl interactions (Supporting Information).

Compounds **3** and **4** are essentially isostructural with **1** except that both are dicationic and one of the phenolic oxygen atoms from the central ligand is not deprotonated. This phenolic –OH group binds to central lanthanide of the {Ln₃} core (Supporting Information). This assignment can be further confirmed by the longer Tb2–O5 and Ho2–O9 bond distances, 2.491(11) and 2.412(8) (Å), respectively, in comparison to bonds formed with phenolate oxygen atoms (Tb(2)–O(9), 2.329(10); Ho(2)–O(5), 2.336(8) (Å); see Supporting Information).

Magnetic Properties. The magnetic susceptibility was measured incorporating our SQUID magnetometer. Since only compound **1** shows a high ground state and a slow relaxation of the magnetization the following discussion will focus on this compound. The magnetic data of **2**, **3**, and **4** is presented in the Supporting Information, Figures S11–S13. Figure 7a depicts susceptibility measurements of **1** plotted as χT vs temperature. The χT value of $41 \text{ cm}^3 \text{ K/mol}$ corresponds well to the theoretical expected value of $40.5 \text{ cm}^3 \text{ K/mol}$, which is expected for three Dysprosium ions with $L = 5$, $S = 2.5$, $J = 7.5$, and $g_j = 1.3$. The square-planar coordinated Ni(II) ions are diamagnetic and are therefore not considered in the description of the magnetic behavior. The decrease at intermediate temperatures can be an indication for weak antiferromagnetic couplings or a strong spin orbit coupling, which is typical for *f*-ions.¹⁸ However, the sharp increase of the susceptibility at low temperatures strongly suggests a high ground state of the effective spin. This is also supported by $M(H)$ measurements at 1.8 K (see Figure 7b).

To quantify the usual model parameters we used an extended Heisenberg–Dirac–van Vleck–Hamiltonian (HDvVH) of the form

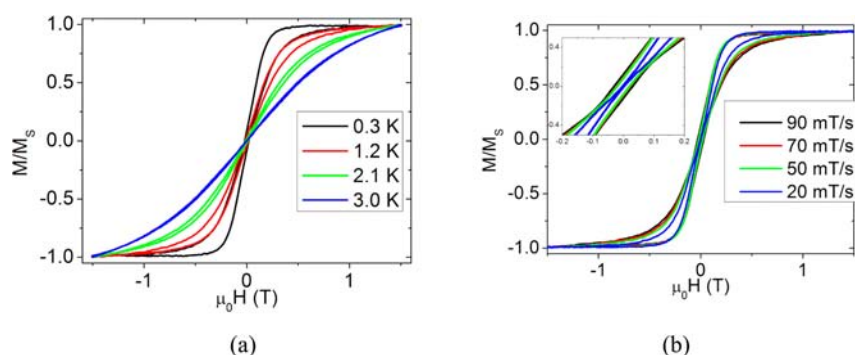


Figure 9. (a) Temperature dependence of the magnetization at a sweep rate of 50 mT/s of **1**; (b) sweep rate dependence at a temperature of 300 mK of **1**, the inset shows a zoom around zero field.

$$\hat{H} = \sum_{i=1}^3 g_i \mu_B \mu_0 \hat{S}_i \mathbf{H} + J_{1,2,3} (\hat{S}_{\text{eff},1} \hat{S}_{\text{eff},2} + \hat{S}_{\text{eff},2} \hat{S}_{\text{eff},3})$$

$$+ D_1 \left(\sum_{i=1,3} \hat{S}_{\text{eff},i,z}^2 - \frac{1}{3} S_{\text{eff},i} (S_{\text{eff},i} + 1) \right)$$

$$+ D_2 \left(\hat{S}_{\text{eff},2,z}^2 - \frac{1}{3} S_{\text{eff},2} (S_{\text{eff},2} + 1) \right)$$

to describe the system. The additional last two terms account the single ion anisotropy of the lanthanide ions. In this model it is assumed, that the D-tensors of the individual ions are approximately collinear. Since in lanthanide ions the spin usually is not a good quantum number we used an effective spin model to account for orbital contributions. The g-factor in this model corresponds to the Landé-factor and can be calculated using Hund's rules. We were able to obtain a best fit with the parameters $g = 1.3$, $J_{1,2,3} = 5$ mK, $D_1 = -21$ K, and $D_2 = -6$ K (See blue line in Figure 7) leading to an effective magnetic ground state of $S_{\text{eff},T} = 15/2$.

To study the dynamic properties of the magnetization we performed variable temperature variable frequency *ac* susceptibility measurements. The results of such a measurement are depicted in Figure 8a and 8b. From this measurements it can be directly concluded that this compound shows a typical SMM behavior with two thermally activated relaxation processes. The high temperature process is dominant in the range between 10 to 17 K and shows a typical Arrhenius like behavior which is expected for a thermal relaxation.¹⁸ The second thermally activated relaxation process can be observed below 7 K. Figure 8c shows the corresponding Arrhenius plot extracted from the *ac* susceptibility data and leads to a value of 85 K for the effective energy barrier U_{eff} and $\tau_0 = 5.9 \times 10^{-7}$ s for the characteristic relaxation time scale at high temperatures, and $U_{\text{eff}} = 53.5$ K, $\tau_0 = 2.3 \times 10^{-8}$ s for low temperatures. The out-of-phase *ac* susceptibility shows a further increase at around 1.8 K, which is nearly temperature independent. This suggests that the driving factor for this relaxation is a quantum tunneling process,¹⁹ which is clearly visible in the Arrhenius plot. From this low temperature part of the relaxation data, the tunnel rate can be roughly estimated to be smaller than 100 s^{-1} (dotted line in Figure 8c). From a frequency dependent analysis of the *ac* susceptibility data with a generalized Debye model (see Supporting Information, Figure S14) an α value of 0.6 for the low temperature and 0.2 for the high temperature relaxation could be obtained. The relatively large value of $\alpha = 0.6$ corresponds to a broad distribution of relaxation times for the

low temperature relaxation. In contrast to this the high temperature relaxation process has a rather narrow distribution. This suggests, that this processes are of different nature.

To further investigate the SMM properties of **1**, we performed additional low temperature magnetization measurements incorporating our homemade Hall probe magnetometer. Figure 9 depicts the results of such a measurement performed on a single crystal.

These measurements clearly reveal a hysteretic behavior up to a blocking temperature of ~ 3 K proving a real SMM behavior of this compound. While at slow sweep rates the hysteresis loops are closed around zero magnetic field they start to open up for sweep rates higher than 50 mT/s (see Figure 9b). This result is consistent with a tunneling rate of $\lesssim 100 \text{ s}^{-1}$ estimated from the *ac* susceptibility.

CONCLUSION

In summary, we have successfully synthesized pentanuclear, both mono and dicationic heterometallic $\{\text{Ni}^{\text{II}}_2\text{Ln}_3\}$ clusters using an unsymmetrically substituted multidentate Schiff base ligand (**LH**₄) generated from 2-aminophenol and 3-((bis(2-hydroxyethyl)amino)methyl)-2-hydroxy-5-methylbenzaldehyde (**C1**). These compounds contain two Ni(II) ions at the two ends and three lanthanides are encapsulated between these two Ni(II) ions. The central $\{\text{Ln}_3\}$ unit arranges almost in a linear fashion. The geometry around the Ni(II) ion is distorted square planar. On the other hand all three Ln(III) ions are octacoordinated, but the central lanthanide has distorted square antiprism geometry while the other two possess trigonal dodecahedron geometry. The magnetic susceptibility measurement shows that compound **1** possesses a ferromagnetic ground state while an antiferromagnetic ground state is observed for **2**, **3**, and **4**. Variable temperature variable frequency *ac* susceptibility measurements reveal that compound **1** shows a typical SMM behavior with at least two relaxation processes. Arrhenius plot extracted from the *ac* susceptibility data leads to an value of 85 K for the effective energy barrier U_{eff} and $\tau_0 = 5.9 \times 10^{-7}$ s for the characteristic relaxation time scale at high temperatures, and $U_{\text{eff}} = 53.5$ K, $\tau_0 = 2.3 \times 10^{-8}$ s for low temperatures. Also an open hysteresis loop up to 3 K was found for **1** with sweep rates faster than 50 mT/s.

ASSOCIATED CONTENT

Supporting Information

Plots and pictures relating to ESI-MS, crystal structures and magnetic studies (Figures S1–S15) and bond parameters

(Tables S1–S5). This material is available free of charge via the Internet at <http://pubs.acs.org>.

AUTHOR INFORMATION

Corresponding Author

*E-mail: vc@iitk.ac.in.

Notes

The authors declare no competing financial interest.

ACKNOWLEDGMENTS

V.C. is thankful to the Department of Science and Technology, India, for a J. C. Bose fellowship. P.B. thanks Council of Scientific and Industrial Research, India, for a Senior Research Fellowship.

REFERENCES

- (1) (a) Sessoli, R.; Powell, A. K. *Coord. Chem. Rev.* **2009**, *253*, 2328. (b) Kahn, O. *Acc. Chem. Res.* **2000**, *33*, 647. (c) Winpenny, R. E. P. *Chem. Soc. Rev.* **1998**, *27*, 447. (d) Kahn, O.; Galy, J.; Journaux, Y. *J. Am. Chem. Soc.* **1982**, *104*, 2165. (e) Pei, Y.; Verdaguer, M.; Kahn, O.; Sletten, J.; Renard, J.-P. *J. Am. Chem. Soc.* **1986**, *108*, 428. (f) Woodruff, D. N.; Winpenny, R. E. P.; Layfield, R. A. *Chem. Rev.* **2013**, *113*, 5110.
- (2) (a) Gatteschi, D.; Fittipaldi, M.; Sangregorio, C.; Sorace, L. *Angew. Chem., Int. Ed.* **2012**, *51*, 4792. (b) Holynska, M.; Premuzic, D.; Jeon, I.-R.; Wernsdorfer, W.; Clerac, R.; Dehnen, S. *Chem.—Eur. J.* **2011**, *17*, 9605. (c) Stamatatos, T. C.; Teat, S. J.; Wernsdorfer, W.; Christou, G. *Angew. Chem., Int. Ed.* **2009**, *48*, 521.
- (3) (a) Osa, S.; Kido, T.; Matsumoto, N.; Re, N.; Pochaba, A.; Mrozinski, J. *J. Am. Chem. Soc.* **2004**, *126*, 420. (b) Chandrasekhar, V.; Dey, A.; Das, S.; Rouzières, M.; Clérac, R. *Inorg. Chem.* **2013**, *52*, 2588. (c) Aronica, C.; Pilet, G.; Chastanet, G.; Wernsdorfer, W.; Jacquot, J. F.; Luneau, D. *Angew. Chem., Int. Ed.* **2006**, *45*, 4659. (d) Novitchi, G.; Wernsdorfer, W.; Chibotaru, L. F.; Costes, J. P.; Anson, C. E.; Powell, A. K. *Angew. Chem., Int. Ed.* **2009**, *48*, 1614. (e) Iasco, O.; Novitchi, G.; Jeanneau, E.; Wernsdorfer, W.; Luneau, D. *Inorg. Chem.* **2011**, *50*, 7373. (f) Okazawa, A.; Nogami, T.; Nojiri, H.; Ishida, T. *Chem. Mater.* **2008**, *20*, 3110. (g) Baskar, V.; Gopal, K.; Helliwell, M.; Tuna, F.; Wernsdorfer, W.; Winpenny, R. E. P. *Dalton Trans.* **2010**, *39*, 4747. (h) Zaleski, C. M.; Depperman, E. C.; Kampf, J. W.; Kirk, M. L.; Pecoraro, V. L. *Inorg. Chem.* **2006**, *45*, 10022. (i) Kajiwara, T.; Nakano, M.; Takaishi, S.; Yamashita, M. *Inorg. Chem.* **2008**, *47*, 8604. (j) Costes, J. P.; Vendier, L.; Wernsdorfer, W. *Dalton Trans.* **2010**, *39*, 4886. (k) Feltham, H. L. C.; Clerac, R.; Powell, A. K.; Brooker, S. *Inorg. Chem.* **2011**, *50*, 4232.
- (4) (a) Shiga, T.; Onuki, T.; Matsumoto, T.; Nojiri, H.; Newton, G. N.; Hoshino, N.; Oshio, H. *Chem. Commun.* **2009**, 3568. (b) Ke, H.; Zhao, L.; Guoa, Y.; Tang, J. *Dalton Trans.* **2012**, *41*, 2314. (c) Saha, A.; Thompson, M.; Abboud, K. A.; Wernsdorfer, W.; Christou, G. *Inorg. Chem.* **2011**, *50*, 10476. (d) Mereacre, V. M.; Ako, A. M.; Clérac, R.; Wernsdorfer, W.; Piloti, G.; Bartolome, J.; Anson, C. E.; Powell, K. A. *J. Am. Chem. Soc.* **2007**, *129*, 9248. (e) Zaleski, C. M.; Depperman, E. C.; Kampf, J. W.; Kirk, M. L.; Pecoraro, V. L. *Angew. Chem., Int. Ed.* **2004**, *43*, 3912. (f) Mereacre, V.; Ako, A. M.; Clérac, R.; Wernsdorfer, W.; Hewitt, I. J.; Anson, C. E.; Powell, A. K. *Chem.—Eur. J.* **2008**, *14*, 3577. (g) Li, M.; Lan, Y.; Ako, A. M.; Wernsdorfer, W.; Anson, C. E.; Buth, G.; Powell, A. K.; Wang, Z.; Gao, S. *Inorg. Chem.* **2010**, *49*, 11587. (h) Mishra, A.; Wernsdorfer, W.; Parson, S.; Christou, G.; Brechin, E. *Chem. Commun.* **2005**, 2086. (i) Papatriantafyllopoulou, C.; Abboud, K. A.; Christou, G. *Inorg. Chem.* **2011**, *50*, 8959. (j) Akhtar, M. N.; Zheng, Y.-Z.; Lan, Y.; Mereacre, V.; Anson, C. E.; Powell, A. K. *Inorg. Chem.* **2009**, *48*, 3502.
- (5) (a) Stoian, S. A.; Paraschiv, C.; Kiritsakas, N.; Lloret, F.; Münck, E.; Bominaar, E. L.; Andruh, M. *Inorg. Chem.* **2010**, *49*, 3387. (b) Nayak, S.; Roubeau, O.; Teat, S. J.; Beavers, C. M.; Gamez, P.; Reedijk, J. *Inorg. Chem.* **2009**, *48*, 216–. (c) Sanz, S.; Ferreira, K.; McIntosh, R. D.; Dalgarno, S. J.; Brechin, E. K. *Chem. Commun.* **2011**, *47*, 9042. (d) Schmidt, S.; Prodius, D.; Mereacre, V.; Kostakis, G. E.; Powell, A. K. *Chem. Commun.* **2013**, *49*, 1696. (e) Schmidt, S.; Prodius, D.; Novitchi, G.; Mereacre, V.; Kostakis, G. E.; Powell, A. K. *Chem. Commun.* **2012**, *48*, 9825. (f) Schray, D.; Abbas, G.; Lan, Y.; Mereacre, V.; Sundt, A.; Dreiser, J.; Waldmann, O.; Kostakis, G. E.; Anson, C. E.; Powell, A. K. *Angew. Chem., Int. Ed.* **2010**, *49*, 5185. (g) Akhtar, M. N.; Mereacre, V.; Novitchi, G.; Tuchagues, J.-P.; Anson, C. E.; Powell, A. K. *Chem.—Eur. J.* **2009**, *15*, 7278–.
- (6) (a) Chandrasekhar, V.; Pandian, B. M.; Vittal, J. J.; Clérac, R. *Inorg. Chem.* **2009**, *48*, 1148. (b) Zheng, Y.-Z.; Evangelisti, M.; Tuna, F.; Winpenny, R. E. P. *J. Am. Chem. Soc.* **2012**, *134*, 1057. (c) Huang, Y.-G.; Wang, X.-T.; Jiang, F.-L.; Gao, S.; Wu, M.-Y.; Gao, Q.; Wei, W.; Hong, M.-C. *Chem.—Eur. J.* **2008**, *14*, 10340. (d) Liu, Y.; Chen, Z.; Ren, J.; Zhao, X.-Q.; Cheng, P.; Zhao, B. *Inorg. Chem.* **2012**, *51*, 7433. (e) Sopasis, G. J.; Orfanoudaki, M.; Zarmpas, P.; Philippidis, A.; Siczek, M.; Lis, T.; O'Brien, J. R.; Milios, C. J. *Inorg. Chem.* **2012**, *51*, 1170. (f) Costes, J.-P.; Vendier, L.; Wernsdorfer, W. *Dalton Trans.* **2011**, *40*, 1700.
- (7) (a) Colacio, E.; Ruiz, J.; Mota, A. J.; Palacios, M. A.; Cremades, E.; Ruiz, E.; White, F. J.; Brechin, E. K. *Inorg. Chem.* **2012**, *51*, 5857. (b) Efthymiou, C. G.; Stamatatos, T. C.; Papatriantafyllopoulou, C.; Tasiopoulos, A. J.; Wernsdorfer, W.; Perlepes, S. P.; Christou, G. *Inorg. Chem.* **2010**, *49*, 9737. (c) Palacios, M. A.; Mota, A. J.; Ruiz, J.; Hänninen, M. M.; Sillanpää, R.; Colacio, E. *Inorg. Chem.* **2012**, *51*, 7010. (d) Papatriantafyllopoulou, C.; Stamatatos, T. C.; Efthymiou, C. G.; Cunha-Silva, L.; Paz, F. A. A.; Perlepes, S. P.; Christou, G. *Inorg. Chem.* **2010**, *49*, 9743. (e) Pointillart, F.; Bernot, K.; Sessoli, R.; Gatteschi, D. *Chem.—Eur. J.* **2007**, *13*, 1602. (f) Pasatou, T. D.; Sutter, J.-P.; Madalan, A. M.; Fellah, F. Z. C.; Duhayon, C.; Andruh, M. *Inorg. Chem.* **2011**, *50*, 5890. (g) Xiong, K.; Wang, X.; Jiang, F.; Gai, Y.; Xu, W.; Su, K.; Li, X.; Yuan, D.; Hong, M. *Chem. Commun.* **2012**, *48*, 7456. (h) Abtab, S. M. T.; Maity, M.; Bhattacharya, K.; Sanudo, E. C.; Chaudhury, M. *Inorg. Chem.* **2012**, *51*, 10211. (i) Wang, H.; Ke, H.; Lin, S.-Y.; Guo, Y.; Zhao, L.; Tang, J.; Li, Y.-H. *Dalton Trans.* **2013**, *42*, 5298.
- (8) (a) Chandrasekhar, V.; Pandian, B. M.; Azhakar, R.; Vittal, J. J.; Clérac, R. *Inorg. Chem.* **2007**, *46*, 5140. (b) Chandrasekhar, V.; Pandian, B. M.; Boomishankar, R.; Steiner, A.; Vittal, J. J.; Hour, A.; Clerac, R. *Inorg. Chem.* **2008**, *47*, 4918.
- (9) (a) Mondal, K. C.; Kostakis, G. E.; Lan, Y.; Wernsdorfer, W.; Anson, C. E.; Powell, A. K. *Inorg. Chem.* **2011**, *50*, 11604. (b) Mondal, K. C.; Sundt, A.; Lan, Y.; Kostakis, G. E.; Waldmann, O.; Ungur, L.; Chibotaru, L. F.; Anson, C. E.; Powell, A. K. *Angew. Chem., Int. Ed.* **2012**, *51*, 7550. (c) Ke, H.; Zhao, L.; Guo, Y.; Tang, J. *Inorg. Chem.* **2012**, *51*, 2699. (d) Nemeč, I.; Machata, M.; Herchel, R.; Boča, R.; Trávníček, Z. *Dalton Trans.* **2012**, *41*, 14603.
- (10) Furniss, B. S.; Hannaford, A. J.; Smith, P. W. G.; Tatchell, A. R. *Vogel's Text book of Practical Organic Chemistry*, 5th ed.; ELBS, Longman: London, U.K., 1989.
- (11) Chandrasekhar, V.; Bag, P.; Colacio, E. *Inorg. Chem.* **2013**, *52*, 4562.
- (12) Azuah, R. T.; Kneller, L. R.; Qiu, Y.; Tregenna-Piggott, P. L. W.; Brown, C. M.; Copley, J. R. D.; Dimeo, R. M. *J. Res. Natl. Inst. Stand. Technol.* **2009**, *114*, 341.
- (13) Das, A.; Gieb, K.; Krupskaya, Y.; Demeshko, S.; Dechert, S.; Klingeler, R.; Kataev, V.; Büchner, B.; Müller, P.; Meyer, F. *J. Am. Chem. Soc.* **2011**, *133*, 3433.
- (14) (a) SMART & SAINT Software Reference manuals, version 6.45; Bruker Analytical X-ray Systems, Inc.: Madison, WI, 2003. (b) Sheldrick, G. M. *SADABS, a software for empirical absorption correction*, version 2.05; University of Göttingen: Göttingen, Germany, 2002. (c) *SHELXTL Reference Manual*, version 6.1; Bruker Analytical X-ray Systems, Inc.: Madison, WI, 2000. (d) Sheldrick, G. M. *SHELXT*, version 6.12; Bruker AXS Inc.: Madison, WI, 2001. (e) Sheldrick, G. M. *SHELXL97, Program for Crystal Structure Refinement*; University of Göttingen: Göttingen, Germany, 1997. (f) Brandenburg, K. *Diamond*, v3.1e; Crystal Impact GbR: Bonn, Germany, 2005.
- (15) (a) Pasteur, L. *Ann. Chim. Phys.* **1848**, *24*, 442. (b) Amouri, H.; Gruselle, M. *Chirality in Transition Metal Chemistry: Molecules*,

Supramolecular Assemblies and Materials; John Wiley & Sons Ltd: Chichester, U.K., 2008.

(16) (a) Chandrasekhar, V.; Bag, P.; Speldrich, M.; Leusen, J. v.; Kögerler, P. *Inorg. Chem.* **2013**, *52*, 5035. (b) Campbell, V. E.; Guillot, R.; Riviere, E.; Brun, P.-T.; Wernsdorfer, W.; Mallah, T. *Inorg. Chem.* **2013**, *52*, 5194.

(17) (a) Mukhopadhyay, A.; Padmaja, G.; Pal, S.; Pal, S. *Inorg. Chem. Commun.* **2003**, *6*, 381. (b) Carrasco, R.; Cano, J.; Ottenwaelder, X.; Aukaaloo, A.; Journaux, Y.; Ruiz-Garcia, R. *Dalton Trans.* **2005**, 2527. (c) Abbas, G.; Lan, Y.; Kostakis, G. E.; Wernsdorfer, W.; Anson, C. E.; Powell, A. K. *Inorg. Chem.* **2010**, *49*, 8067. (d) Gamez, P.; Zhao, L.; Lin, S. Y.; Deng, R. P.; Tang, J. K.; Zhang, H. J. *J. Am. Chem. Soc.* **2010**, *132*, 8538.

(18) Lin, P.-H.; Burchell, T. J.; Ungur, L.; Chibotaru, L. F.; Wernsdorfer, W.; Murugesu, M. *Angew. Chem., Int. Ed.* **2009**, *48*, 9489.

(19) Gatteschi, D.; Sessoli, R.; Villain, J. *Molecular nanomagnets*; Oxford University Press: Oxford, U.K., 2006.